Please cite this article in press as: Pan et al., *C. elegans* AP-2 and Retromer Control Wnt Signaling by Regulating MIG-14/Wntless, Developmental Cell (2008), doi:10.1016/j.devcel.2007.12.001

Developmental Cell
Short Article

C. elegans AP-2 and Retromer Control Wnt Signaling by Regulating MIG-14/Wntless

Chun-Liang Pan,[1] Paul D. Baum,[1,5] Mingyu Gu,[2,3] Erik M. Jorgensen,[2,3] Scott G. Clark,[4,6] and Gian Garriga[1,*]
[1]Helen Wills Neuroscience Institute, Department of Molecular and Cell Biology, University of California, Berkeley, Berkeley, CA 94720-3204, USA
[2]Howard Hughes Medical Institute
[3]Department of Biology
University of Utah, Salt Lake City, UT 84112, USA
[4]Molecular Neurobiology Program, Department of Pharmacology, Skirball Institute, New York University School of Medicine, New York, NY 10016, USA
[5]Present address: Division of Experimental Medicine, Department of Medicine, San Francisco General Hospital, University of California, San Francisco, San Francisco, CA 94110, USA.
[6]Present address: Biology Department, University of Nevada, Reno, NV 89557, USA.
*Correspondence: garriga@berkeley.edu
DOI 10.1016/j.devcel.2007.12.001

SUMMARY

While endocytosis can regulate morphogen distribution, its precise role in shaping these gradients is unclear. Even more enigmatic is the role of retromer, a complex that shuttles proteins between endosomes and the Golgi apparatus, in Wnt gradient formation. Here we report that DPY-23, the *C. elegans* μ subunit of the clathrin adaptor AP-2 that mediates the endocytosis of membrane proteins, regulates Wnt function. *dpy-23* mutants display Wnt phenotypes, including defects in neuronal migration, neuronal polarity, and asymmetric cell division. DPY-23 acts in Wnt-expressing cells to promote these processes. MIG-14, the *C. elegans* homolog of the Wnt-secretion factor Wntless, also acts in these cells to control Wnt function. In *dpy-23* mutants, MIG-14 accumulates at or near the plasma membrane. By contrast, MIG-14 accumulates in intracellular compartments in retromer mutants. Based on our observations, we propose that intracellular trafficking of MIG-14 by AP-2 and retromer plays an important role in Wnt secretion.

INTRODUCTION

During development, morphogens control pattern formation by specifying individual cell fates along their gradients (Tabata and Takei, 2004). These graded signaling molecules can also function as guidance cues by providing instructive information for migrating cells and axon growth cones (Zou and Lyuksyutova, 2007). Over the years, many morphogens and guidance cues have been identified, yet how gradients of these molecules are produced and shaped is often mysterious.

Wnts are a family of secreted glycoproteins that have been shown to act as classical morphogens (Zecca et al., 1996). Wnts can also function as guidance cues to control the migrations of axon growth cones in *C. elegans, Drosophila*, and the vertebrate central nervous system (Liu et al., 2005; Lyuksyutova et al., 2003; Pan et al., 2006; Yoshikawa et al., 2003). In *C. elegans*, Wnts also act as positional cues to control the asymmetric divisions of the T and EMS blast cells (Goldstein et al., 2006).

Two classes of molecules have recently been shown to function in Wnt-secreting cells to produce a functional Wnt. The first are components of the retromer complex. Retromer retrieves from endosomes receptors that shuttle vacuolar or lysosomal hydrolases, returning the receptors to the Golgi (Seaman, 2005; Seaman et al., 1998). *C. elegans* homologs of Vps26p, Vps29p, and Vps35p, components in the retromer complex, are necessary for several developmental processes that require Wnts, and VPS-35 has been shown to function in cells that produce the Wnt EGL-20 (Coudreuse et al., 2006; Prasad and Clark, 2006).

Three groups have found a new molecule known as Wntless, Evi, or Sprinter, that is necessary for Wnt function (Banziger et al., 2006; Bartscherer et al., 2006; Goodman et al., 2006). Wntless interacts physically with Wingless, targeting it to the cell surface for secretion (Banziger et al., 2006). *C. elegans* MIG-14, which is also known as MOM-3, is the homolog of Wntless (Banziger et al., 2006). The *mig-14* alleles were originally identified in screens for mutants with defects in QL migration, which the Wnt EGL-20 regulates (Harris et al., 1996; Maloof et al., 1999). A screen for mutants with defects in the asymmetric division of the EMS blast cell identified the original *mom-3* allele. MOM-3 acts in P2, the cell that secretes the Wnt MOM-2 and signals to EMS, causing it to divide asymmetrically (Thorpe et al., 1997).

In this paper, we establish a connection between endocytosis, retromer function, and MIG-14. The *C. elegans* gene *dpy-23* encodes the μ subunit of the AP-2 clathrin adaptor complex that is necessary for receptor-mediated endocytosis and functions in several Wnt-related processes. Our observations indicate that efficient Wnt secretion requires endocytosis and trafficking of MIG-14 by retromer.

RESULTS

dpy-23 Mutants Display Wnt Phenotypes

During embryogenesis, the two HSN neurons migrate anteriorly from the tail to positions near the middle of the embryo (Sulston

Please cite this article in press as: Pan et al., *C. elegans* AP-2 and Retromer Control Wnt Signaling by Regulating MIG-14/Wntless, Developmental Cell (2008), doi:10.1016/j.devcel.2007.12.001

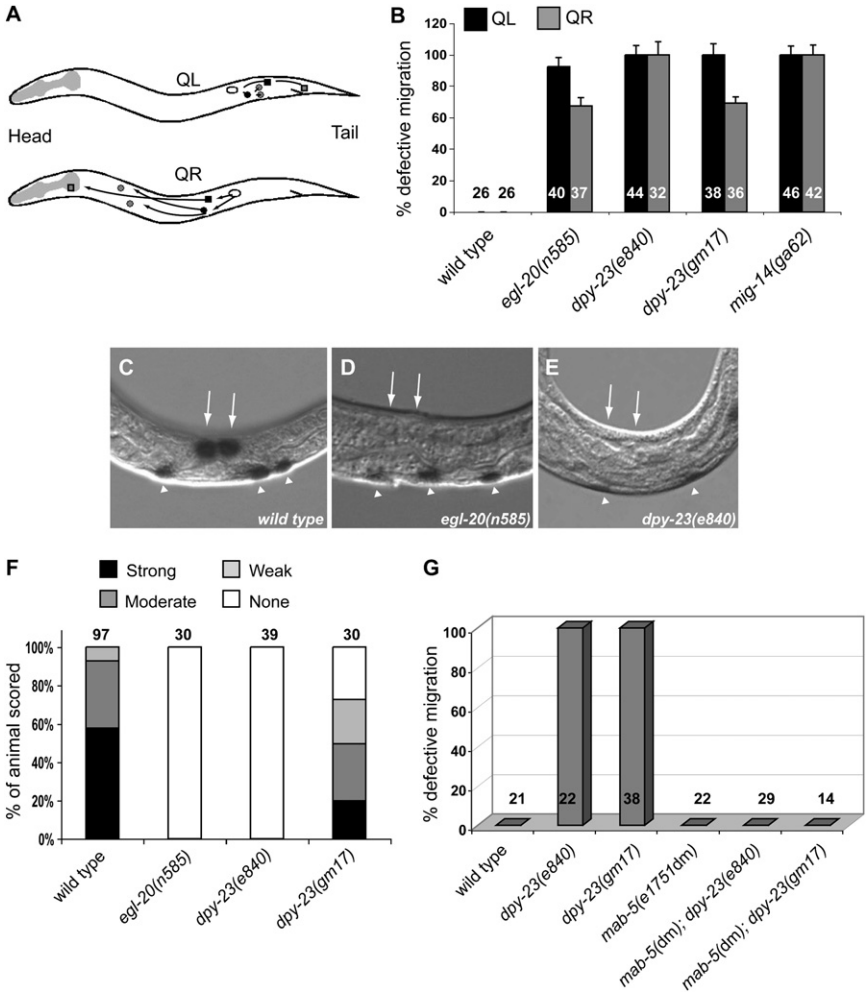

Figure 1. *dpy-23* Regulates QL Migration by Transcriptionally Activating the Wnt Target Gene *mab-5*

(A) Schematic diagram of left and right lateral views of a first larval stage animal showing the migrations of the QL and QR descendents, respectively. Filled squares, QL.a and QR.a; filled circles, QL.p and QR.p; shaded squares, PQR (left side) and AQR (right side); shaded circles, PVM and SDQL (left side), and AVM and SDQR (right side).

(B) Graph shows the percentage (with SEM) of QL and QR descendents that are migration-defective. In (B), (F), and (G), numbers of cells scored for each genotype are provided.

(C–E) β-galactosidase activity in wild-type (C), *egl-20* (D), and *dpy-23* (E) animals with the integrated array *muIs3[Pmab-5::lacZ]*. Arrows indicate the positions of the QL neuroblast daughters and arrowheads indicate the positions of motor neurons that express β-galactosidase.

(F) Graph shows quantification of *mab-5* transcriptional activity. Intensity of β-galactosidase activity in the Q lineage was classified into four categories: strong, moderate, weak, or no staining.

(G) Graph shows the percentage of defective migrations of the QL descendents for each genotype.

et al., 1983). In a screen for mutants with defective HSN migration, we isolated *dpy-23(gm17)*. The HSNs were usually displaced posteriorly in the mutant, migrating only part of the distance from the tail to their normal destinations (Figure S1, see the Supplemental Data available with this article online). The mutant also had a squat body stature that is referred to as the Dumpy (Dpy) phenotype. The mutation mapped to the same region of the X chromosome as *dpy-23* and failed to complement *dpy-23(e840)*. Both *e840* and *gm17* mutants displayed Dpy, HSN, and several other phenotypes that are described below. All of these phenotypes were maternally and zygotically rescued: only homozygous mutants of homozygous mothers exhibited the mutant phenotypes.

Several Wnts contribute to HSN migration (Pan et al., 2006; Figure S1), and further phenotypic analysis revealed that *dpy-23* mutants exhibited a number of other phenotypes shared by Wnt mutants. In the first larval stage (L1), the left Q neuroblast (QL) and its descendents migrate posteriorly, while the right Q neuroblast (QR) and its descendents migrate anteriorly (Figure 1A; Sulston and Horvitz, 1977). Loss of the Wnt EGL-20, the Frizzled receptors MIG-1 or LIN-17, the Dishevelled MIG-5, the β-catenin BAR-1, or the TCF transcription factor POP-1 cause the QL descendents to migrate anteriorly (Harris et al., 1996; Herman, 2001; Maloof et al., 1999; Walston et al., 2006). The two mutations in *dpy-23* caused a similar phenotype (Figure 1B).

The Wnt EGL-20 and its downstream effectors direct QL migration by activating transcription of the Hox gene *mab-5* (Maloof et al., 1999). Animals with compromised EGL-20 signaling display diminished expression of *mab-5* in QL and its descendents. Using a *Pmab-5::lacZ* reporter, we found that *dpy-23* mutants also had attenuated β-galactosidase expression in QL and its descendents (Figures 1C–1F). The effects of the *e840* mutation were more severe than those caused by *gm17*.

Consistent with the hypothesis that *dpy-23* regulates *mab-5* expression in QL, the gain-of-function *mab-5* mutation *e1751*dm completely suppressed the QL migration defects of *dpy-23* mutants (Figure 1G). This allele causes expression of *mab-5* in the absence of Wnt signaling and suppresses the QL defects of Wnt signaling mutants (Maloof et al., 1999). Taken together, these results suggest that DPY-23 regulates the migrations of the QL descendents through *mab-5*, the target gene for EGL-20/Wnt.

The *dpy-23* mutants displayed several other Wnt phenotypes. Loss of either of the two Wnts, EGL-20 or CWN-1, causes QR and its descendents to terminate their anterior migrations prematurely (Harris et al., 1996; C.-L.P. and G.G., unpublished data). The *dpy-23* mutations caused a similar QR phenotype that was more severe than either single Wnt mutant but similar to the *cwn-1; egl-20* double mutant (Figure 1B and data not shown).

In addition to cell migration, Wnt signaling controls the polarity of neurons and nonneural cells. The mechanosensory neuron ALM extends a single anterior process in wild-type animals (White et al., 1986; Figure 2A). While ALM neuronal polarity is

Please cite this article in press as: Pan et al., *C. elegans* AP-2 and Retromer Control Wnt Signaling by Regulating MIG-14/Wntless, Developmental Cell (2008), doi:10.1016/j.devcel.2007.12.001

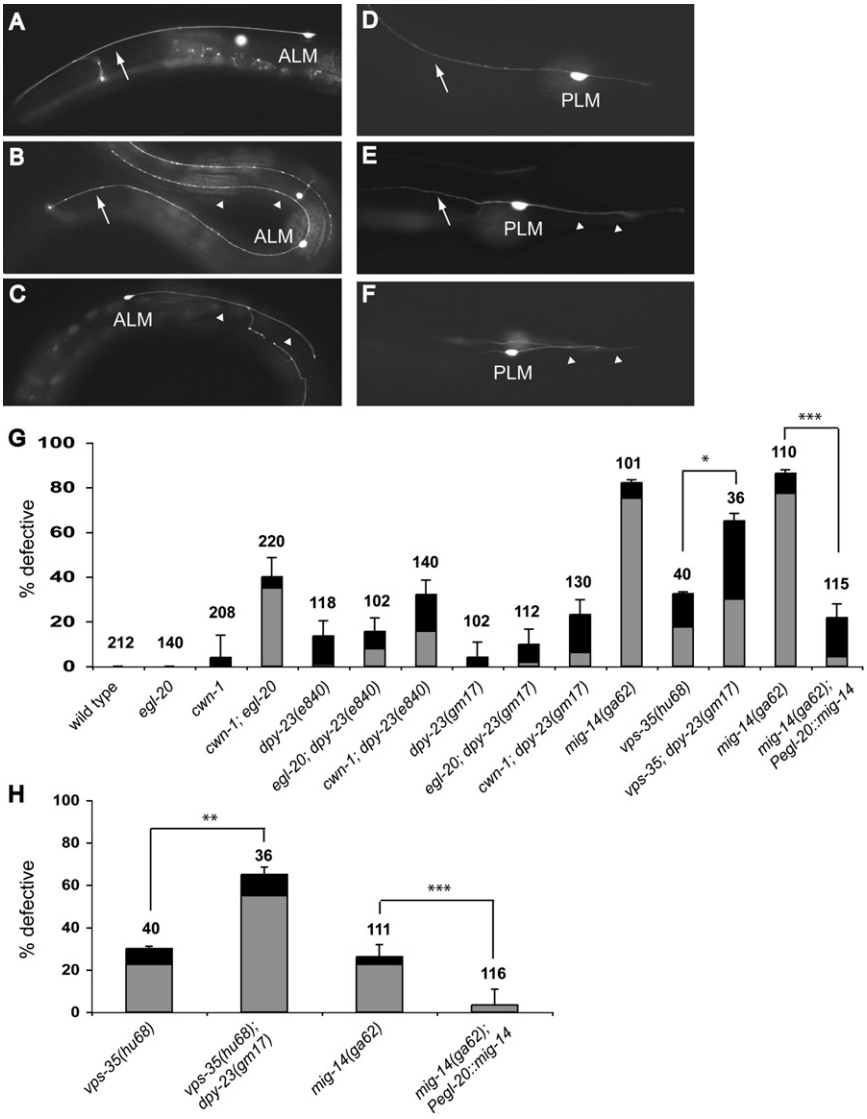

Figure 2. *dpy-23*, *mig-14*, and *vps-35* Mutants Display Defective ALM and PLM Neuronal Polarity

(A–F) Photomicrographs showing ALM (A–C) and PLM (D–F) neuronal morphology. The ALM and PLM cell bodies are labeled. Anterior processes are indicated by arrows and posterior processes by arrowheads. (A) Wild-type ALM with a single, anterior process.

(B) Bipolar ALM with a normal anterior process and an ectopic posterior process.

(C) ALM with a single posterior process, indicating a reversal of polarity.

(D) Wild-type PLM with a long anterior process and a short posterior process.

(E) PLM with symmetric polarity. The cell has a normal anterior process and a long posterior process.

(F) PLM with reversed polarity. The anterior process is short, and the abnormally long posterior process folds back on itself at the tip of the tail and projects anteriorly.

(G and H) Graph shows the percentage (with SEM) of ALM (G) and PLM (H) neurons with defective polarity for each genotype. Black bars indicate the bipolar phenotype and gray bars indicate reversed polarity. Numbers of axons scored for each genotype are provided. *$p < 0.05$; **$p < 0.01$; ***$p < 0.001$ (Fisher's exact test).

normal in *egl-20*, *cwn-1*, or *cwn-2* single mutants, the ALMs of *cwn-1; egl-20* and *cwn-1; cwn-2* double mutants are often bipolar or have reversed axonal polarity (Figures 2B, 2C, and 2G; Hilliard and Bargmann, 2006; Prasad and Clark, 2006). In *dpy-23* mutants, the ALMs occasionally extended processes posteriorly, and this phenotype was enhanced by a *cwn-1* mutation (Figure 2G). The ALM and QR defects suggest that *dpy-23* functions with multiple Wnts.

The V5 cells normally divide asymmetrically to produce an anterior cell that joins the hypodermal syncytium and a posterior blast cell (Sulston and Horvitz, 1977). In *egl-20* mutants, the division is occasionally reversed to produce an anterior blast cell and a posterior syncytial cell (Whangbo et al., 2000), a phenotype that we found was enhanced by a *cwn-1* mutation (Figure S2). *dpy-23* mutants also displayed this phenotype (Figure S2).

The phenotypic similarities between *dpy-23* and Wnt mutants argue that DPY-23 regulates Wnt signaling. Developmental processes controlled by other signaling pathways, such as neuronal and growth cone migrations that are regulated by the guidance cues UNC-6/Netrin and SLT-1/Slit, appeared normal in *dpy-23* mutants (data not shown). While DPY-23 regulates the EGF receptor in vulval development (Yoo and Greenwald, 2005), the lack of many signaling phenotypes in *dpy-23* mutants suggests that DPY-23 plays a relatively specific role in Wnt signaling.

dpy-23 Encodes the *C. elegans* Homolog of the μ2 Subunit of the AP-2 Complex

Genetic mapping and transformation rescue of *dpy-23* showed that it encodes the *C. elegans* ortholog of the μ subunit of the AP-2 complex (data not shown). The *e840* allele is a large deletion removing the entire *dpy-23* gene and flanking sequences. The *gm17* allele is a splice donor site mutation in the last intron and is predicted to truncate the C-terminal 40 amino acids of the protein. Since the phenotypes of *e840* are generally more severe than *gm17* animals, we speculate that either the severity of the *e840* phenotypes results from the removal of additional genes by the *e840* deletion or the *gm17* mutation does not eliminate *dpy-23* function. We expressed a genomic *dpy-23* fragment tagged with GFP at the C terminus in *e840* mutant animals and found that the mutant phenotypes were completely rescued, suggesting that the adjacent genes deleted in *e840* do not contribute significantly to the *dpy-23* phenotypes (Figure 3A and data not shown).

Please cite this article in press as: Pan et al., *C. elegans* AP-2 and Retromer Control Wnt Signaling by Regulating MIG-14/Wntless, Developmental Cell (2008), doi:10.1016/j.devcel.2007.12.001

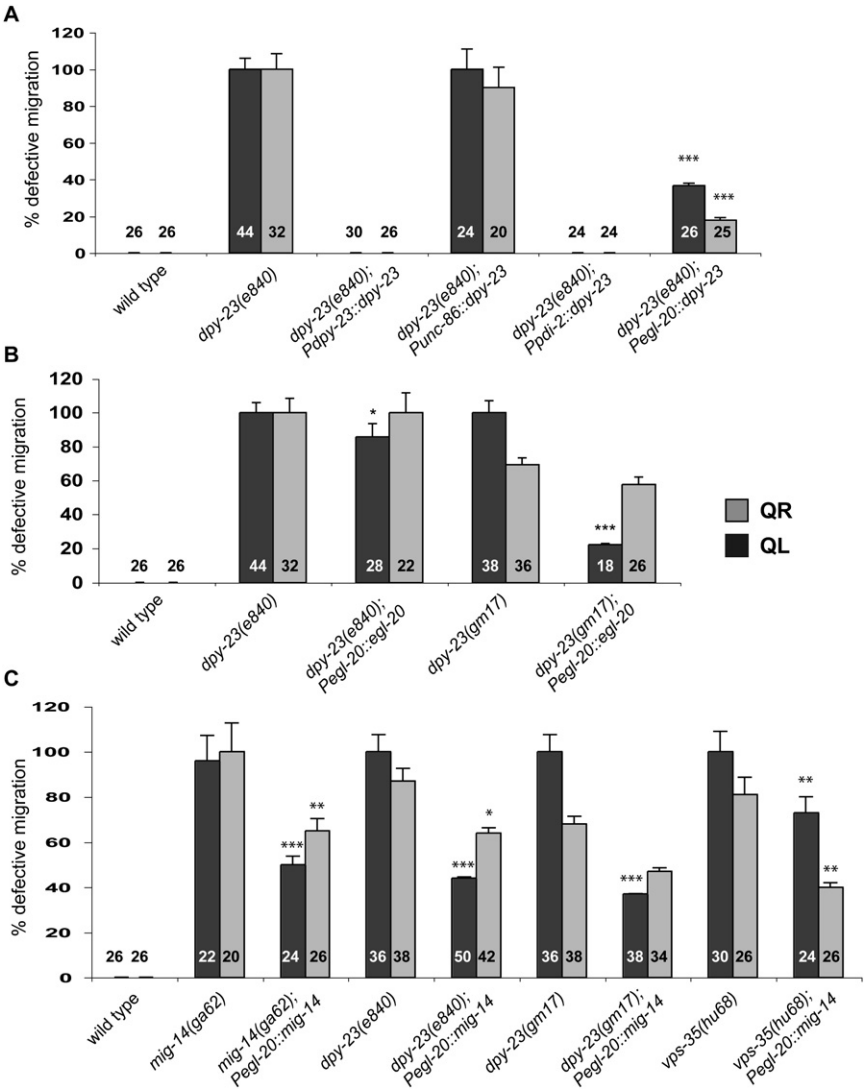

Figure 3. *dpy-23* and *mig-14* Function in EGL-20/Wnt-Secreting Cells

(A–C) Numbers of cells scored for each genotype are provided.

(A) Graph shows the percentage (with SEM) of neuronal migration defects in *dpy-23(e840)* mutants expressing *dpy-23* from the endogenous *dpy-23*, the neuronal *unc-86*, the hypodermal *pdi-2*, and the *egl-20* promoters.

(B) Effects of excess EGL-20 on the migrations of QL and QR descendents in *dpy-23* mutants.

(C) Effects of MIG-14 expression on the Q migration defects of *mig-14(ga62), dpy-23(e840), dpy-23(gm17)*, and *vps-35(hu68)* mutants. *$p < 0.05$; **$p < 0.01$; ***$p < 0.001$ (Fisher's exact test).

dpy-23 Functions in Wnt-Producing Cells

To determine where DPY-23 functions, we expressed a *dpy-23* cDNA fused to GFP from tissue-specific promoters and asked whether these transgenes rescued the defects of *dpy-23* mutants. Expression of DPY-23::GFP in the HSN and Q descendents from the neuronal specific *unc-86* promoter failed to rescue the neuronal migration defects (Figure 3A and Figure S1). We previously used this promoter to express a cDNA for the Frizzled receptor MIG-1 and showed that it could rescue the HSN defects of a *mig-1* mutant (Pan et al., 2006). Expression of DPY-23::GFP in hypodermal cells from the *pdi-2* promoter, by contrast, completely rescued the Q defects and partially rescued the HSN defects of *dpy-23* mutants (Figure 3A and Figure S1). The *pdi-2* and *dpy-23* promoters are active in the B, F, K, and U hypodermal cells that also produce the Wnt EGL-20 (Figure S3), raising the possibility that *dpy-23* could function in EGL-20-producing cells. Consistent with this hypothesis, expression of DPY-23::GFP from the *egl-20* promoter partially rescued the Q and HSN defects, suggesting that DPY-23 functions in Wnt-producing cells (Figure 3A and Figure S1). The lack of complete rescue for the HSN and QR phenotypes might be explained by the requirement for multiple Wnts that function in these migrations (Pan et al., 2006; C.-L.P. and G.G., unpublished data).

Genetic Interactions between *dpy-23*, *vps-35*, and *mig-14*

Several recently identified proteins also regulate the production of functional Wnts. Homologs of Vps35p, Vps26p, and Vps29p, subunits of the yeast retromer complex responsible for the trafficking of proteins between the Golgi and endosomes (Seaman et al., 1998), regulate Wnt function in *C. elegans* (Coudreuse et al., 2006; Prasad and Clark, 2006). *C. elegans vps-35* mutants display Wnt phenotypes, including defects in neuronal migrations and polarity, and the *egl-20* phenotypes displayed by *vps-35* mutants were rescued by expression of VPS-35 in cells that produce EGL-20.

Wntless, also known as Evi or Sprinter, was identified in *Drosophila* as a membrane protein required for Wnt secretion (Banziger et al., 2006; Bartscherer et al., 2006; Goodman et al., 2006). Mutations in the *C. elegans* homolog of Wntless MIG-14, also known as MOM-3, disrupt the asymmetric divisions of EMS and V5 and the migrations of the HSNs and Q neuroblasts, resulting in mutant phenotypes similar to those caused by mutations in the Wnt genes *mom-2* or *egl-20* (Harris et al., 1996; Thorpe et al., 1997; Whangbo et al., 2000). We will refer to the *Drosophila* homolog as Wntless and the *C. elegans* homolog as MIG-14.

We analyzed the phenotypes caused by four *mig-14* alleles. Both *or78* and *gm2* resulted in maternal-effect lethality, whereas *ga62* and *mu71* were viable as homozygous strains. All four alleles caused HSN and Q migration defects (Figure S1 and data not shown), and our observations suggest that *or78* and *gm2* alleles severely reduce or eliminate *mig-14* activity. *ga62* and

mu71 alleles only partially disrupt *mig-14* function, with *mu71* being weaker. We focused on *ga62* for the experiments described below.

In addition to neuronal migration defects, we also discovered ALM polarity defects in *mig-14(ga62)* mutants. *mig-14* mutants also had defects in PLM polarity, a phenotype displayed by *lin-44* Wnt mutants (Figure 2). Each PLM neuron extends a single anterior process and a very short posterior process (Figure 2D). In *lin-44*, *vps-26, vps-35*, or *mig-14* mutants, the PLMs extended a short anterior process and a long posterior process, a reversal in polarity (Figures 2E and 2F; Hilliard and Bargmann, 2006; Prasad and Clark, 2006). *mig-14* mutations also reverse the polarity of the V5 division (Figure S2; Whangbo et al., 2000). These results confirm and extend previous descriptions of *mig-14* mutant phenotypes, and they suggest that MIG-14 regulates Wnt signaling in *C. elegans*.

To investigate genetic interactions among these genes, we attempted to construct double mutant combinations. *mig-14; dpy-23* and *vps-35(hu68); dpy-23(e840)* double mutants were not viable, precluding us from further analysis. Homozygous *vps-35(hu68); dpy-23(gm17)* animals from *vps-35(hu68)/+; dpy-23(gm17)* mothers, however, retain the maternal contribution of *vps-35* and although extremely sick and sterile, they are viable. Both the *vps-35* ALM and PLM polarity defects were significantly enhanced in the *vps-35(hu68); dpy-23(gm17)* double mutant compared to either single mutant (Figures 2G and 2H). Enhancement of the PLM defects reveals a role for DPY-23 in PLM polarity that was not apparent in *dpy-23* single mutants.

The Subcellular Localization of MIG-14 Depends on DPY-23 and Retromer

EGL-20/Wnt is expressed at similar levels in wild-type, *dpy-23*, and *mig-14* animals, indicating that *dpy-23* or *mig-14* does not regulate Wnt expression (Figure S4). The *egl-20* translational GFP reporter used had been shown to fully rescue the neuronal defects of *egl-20* mutants (Whangbo and Kenyon, 1999), and we previously showed that it caused excessive HSN migration in sensitized genetic backgrounds, indicating a high level of expression (Pan et al., 2006). This reporter was able to rescue most of the QL defects of the *dpy-23(gm17)* mutant, and also a small but significant percentage of QL defects of the *dpy-23(e840)* mutant (Figure 3B). However, it failed to rescue the HSN and QR defects of either allele (Figure 3B and data not shown). The ability of excess EGL-20 to rescue the QL migration defects of *dpy-23* mutants may reflect the fact that EGL-20 is the sole Wnt involved in QL migration and hence plays a more prominent role than it does in the QR and HSN migrations.

The discovery of Wntless as a component required for Wingless secretion suggested that endocytosis could be necessary for the recycling of the Wntless protein. We examined the subcellular distributions of MIG-14 in EGL-20/Wnt-producing cells (Figure 4). A translational GFP fusion of *mig-14* was expressed under the control of the *egl-20* promoter. We first observed MIG-14::GFP expression in the 1.5-fold embryo, and it continued through all larval and adult stages, consistent with previous reports on the temporal profile of *egl-20* promoter activity (data not shown; Pan et al., 2006; Whangbo and Kenyon, 1999). The MIG-14::GFP fusion protein was functional: when expressed in EGL-20/Wnt-secreting cells, it partially rescued the HSN and Q neuroblast migration defects and the ALM and PLM neuronal polarity defects of *mig-14* mutants, indicating that it acts in Wnt-secreting cells (Figures 2G, 2H, and 3C, and Figure S5; Banziger et al., 2006; Thorpe et al., 1997). Epifluorescence (Figure 4A) and confocal imaging (Figure 4D) of MIG-14::GFP in living animals showed that MIG-14::GFP localized to the cell periphery and intracellular compartments (Figures 4A, 4D, and 4G).

MIG-14::GFP localization changed in *dpy-23* and *vps-35* mutants. MIG-14::GFP accumulated at or near the plasma membrane in *dpy-23* mutants (Figures 4B and 4G, and Figure S6). We often observed MIG-14::GFP to be in large vesicular structures closely associated with the cell membrane (Figure 4E). These vesicles were never seen in retromer mutants, and were only infrequently observed in *mig-14* mutants. In *vps-35* mutants, by contrast, MIG-14::GFP accumulated in discrete intracellular structures that were absent in control animals, and it rarely localized to the cell periphery (Figures 4C, 4F, and 4G, and Figure S6). Moreover, we observed a significant decrease in MIG-14 levels in *vps-35* mutants (Figures 4H–4J), suggesting that in the absence of retromer function, MIG-14 may be targeted for degradation.

These results suggest that DPY-23 and VPS-35 control Wnt secretion by regulating MIG-14 recycling. A prediction of this model is that excess MIG-14 should at least partially bypass the requirement for DPY-23 and VPS-35. Consistent with this model, expression of excess MIG-14 in Wnt-secreting cells rescued the QL, QR, and HSN defects of *dpy-23* and *vps-35* mutants (Figure 3C and Figure S5). By contrast, expression of excess DPY-23 in Wnt-secreting cells failed to rescue the neuronal defects of *mig-14* mutants (data not shown).

DISCUSSION

Wnt function requires the *C. elegans* AP-2 μ subunit DPY-23. Together with retromer, DPY-23 regulates the intracellular distribution of MIG-14, a Wnt-binding factor required for Wnt secretion. We speculate that newly synthesized EGL-20/Wnt binds to MIG-14 in the Golgi, targeting the Wnt to the cell membrane for secretion. In this model, AP-2-mediated endocytosis and retromer retrieval at the sorting endosome would recycle MIG-14 to the Golgi, where it can bind to EGL-20/Wnt for next cycle of secretion.

Studies in *Drosophila* demonstrated a role for endocytosis in the formation of a Wingless gradient. Models based on a nonautonomous requirement for dynamin in Wnt function implicated endocytosis as part of a relay that transferred Wingless from one cell to the next (Bejsovec and Wieschaus, 1995; Moline et al., 1999). Other investigators proposed that the Wingless gradient was generated by diffusion. These investigators proposed that the effects of dynamin loss on Wnt function reflected a lack of Wingless secretion from cells expressing the morphogen (Strigini and Cohen, 2000). While our results do not directly resolve this controversy, the requirement for DPY-23 in MIG-14 endocytosis supports the hypothesis that endocytosis is necessary for Wnt secretion and provides a mechanism for how endocytosis regulates Wnt secretion.

A previous study argued that retromer was not necessary for Wnt secretion, but instead was necessary for production of a functional Wnt (Coudreuse et al., 2006). These investigators

Please cite this article in press as: Pan et al., *C. elegans* AP-2 and Retromer Control Wnt Signaling by Regulating MIG-14/Wntless, Developmental Cell (2008), doi:10.1016/j.devcel.2007.12.001

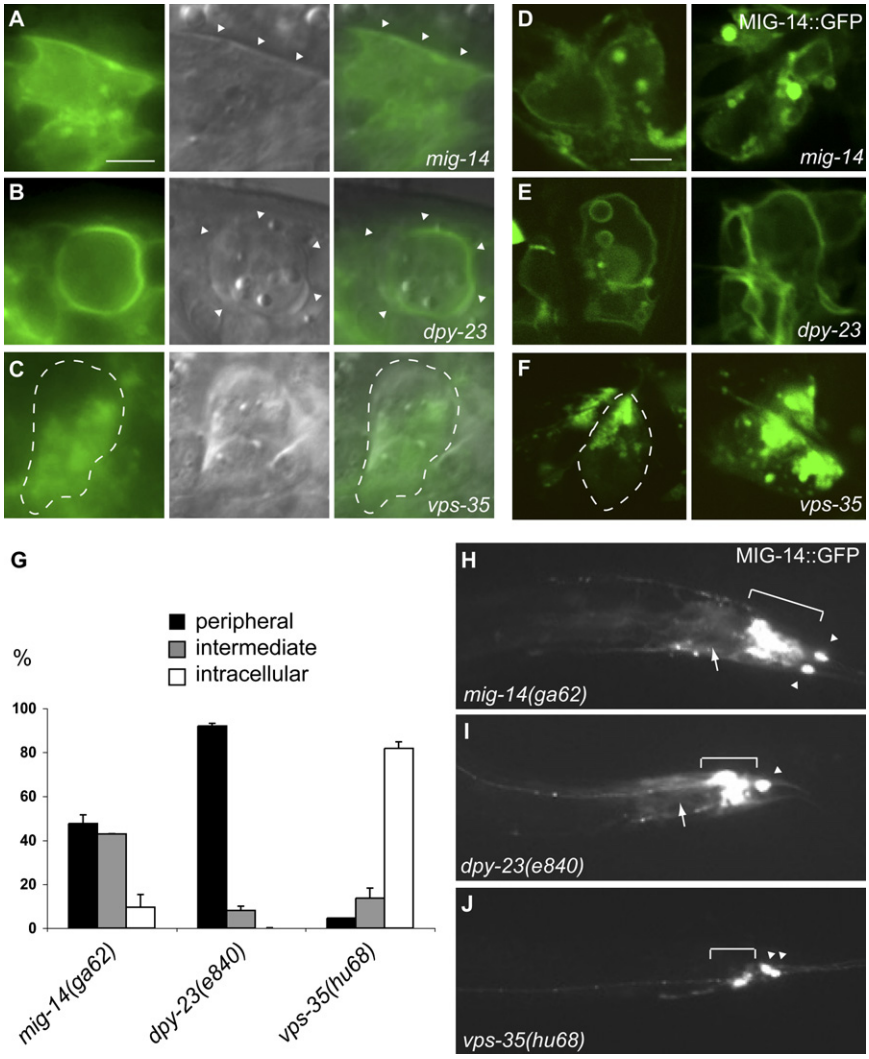

Figure 4. Subcellular Localization of MIG-14 Requires DPY-23 and VPS-35

(A–C) Epifluorescence and Nomarski images of a translational MIG-14::GFP fusion protein expressed in EGL-20 secreting cells of living animals. Left, GFP epifluorescence; middle, Nomarski images; right, overlay. Arrowheads (A and B) or dashed lines (C) mark cell boundaries. To eliminate endogenous MIG-14, we expressed MIG-14::GFP in *mig-14(ga62)* mutants and used this strain as a control.

(A) *mig-14(ga62)*: MIG-14::GFP was localized at or near the plasma membrane and in intracellular compartments.

(B) *dpy-23(e840)* mutant: MIG-14::GFP accumulated at or near the plasma membrane.

(C) *vps-35(hu68)* mutant: MIG-14::GFP accumulated in intracellular compartments and was significantly decreased from the cell periphery.

(D–F) Representative confocal images of various MIG-14::GFP patterns in living animals. We classified MIG-14::GFP distribution into three categories: (D) intermediate pattern, where MIG-14::GFP is both at the cell periphery and in the intracellular compartments; (E) peripheral pattern, where MIG-14::GFP is predominantly at the cell periphery; and (F) intracellular pattern, where MIG-14::GFP is localized to intracellular compartments with little or no signal at the cell periphery.

(G) The distribution of MIG-14::GFP was quantified from single confocal sections through the center of the GFP-expressing cells. Four lines of fluorescence intensity, one horizontal, one vertical, and two diagonal, were scanned. A peripheral distribution was defined when the fluorescence intensity on the cell membrane was more than 2-fold the highest intracellular fluorescence intensity in three out of the four measurements (Figure S6A). An intracellular distribution was defined when the peak intracellular fluorescence intensity was more than 2-fold the fluorescence intensity on the cell membrane in three out of the four measurements (Figure S6C). Distributions other than those described above were defined as an intermediate distribution (Figure S6B). Graph shows the percentage (with SEM) of different MIG-14::GFP distributions in *mig-14(ga62)*, *dpy-23(e840)*, and *vps-35(hu68)* mutants. Total numbers of cells scored: *mig-14(ga62)*, 21; *dpy-23(e840)*, 25; *vps-35(hu68)*, 44.

(H–J) Epifluorescence photomicrographs showing the tails of the larvae (anterior is to the left and dorsal is up). In *vps-35(hu68)* but not in the *dpy-23(e840)* mutants, the level of MIG-14::GFP often decreased significantly. Camera settings were the same for all three genotypes. Brackets indicate the location of hypodermal cells expressing MIG-14::GFP. Intestinal muscles which are immediately anterior to these cells also expressed this transgene at a much lower level (arrows). Arrowheads indicate PLM neurons marked by the integrated GFP reporter *zdIs5[Pmec-4::gfp]*. Scale bar = 5 μm.

also proposed that retromer was necessary for long-range Wnt signaling, but only played a minor role in short-range signaling. They argued that retromer mutants produced Wnt molecules that could only act on nearby cells but failed to act on more distant cells. Our findings that retromer is required for MIG-14 trafficking and the previous discovery that Wntless, the *Drosophila* MIG-14 homolog, is necessary for Wingless secretion are at odds with the interpretation that retromer plays a specific role in production of a Wnt that acts in long-range signaling (Banziger et al., 2006; Bartscherer et al., 2006).

An argument for retromer playing a specific role in long-range signaling was based on the observations that retromer mutants have little effect on processes that require MOM-2 and LIN-44, Wnts that are produced near responding cells (Coudreuse et al., 2006). Further support for the long-range hypothesis was based on the higher frequency of V5 defects in *egl-20* mutants compared to retromer mutants (Coudreuse et al., 2006). This difference contrasted with the high frequency of QL migration defects in both *egl-20* and retromer mutants. The discrepancy between the V5 and QL defects in the two types of mutants was explained by the closer proximity of the V5 cell to the EGL-20 source. The model that retromer plays a specific role in long-range Wnt signaling has led to speculation that the trafficking events regulated by this complex might control the production of a specifically modified form of Wnt (Coudreuse and Korswagen, 2007; Coudreuse et al., 2006; Hausmann et al., 2007), for example, a Wnt that could associate with lipoprotein particles (Panakova et al., 2005).

We favor a simpler hypothesis where retromer is required for MIG-14 recycling and where blocked recycling leads to defects in Wnt secretion. Our observation that excess MIG-14 can ameliorate the Wnt phenotypes of *dpy-23* and *vps-35* mutants is consistent with the notion that low levels of functional Wnts are still secreted in these mutants. We propose that the phenotypic differences observed between retromer and *egl-20* mutants may result from differential sensitivities of various responding cells to lowered Wnt levels, and a similar explanation could account for the phenotypic differences between *dpy-23* and Wnt mutants.

While the phenotypes of *mig-14* mutants have most of the defects displayed by either single Wnt mutants or Wnt mutant combinations, *dpy-23* mutants do not exhibit certain Wnt mutant phenotypes. They do not have the severe ALM polarity defects that are exhibited by *cwn-1; egl-20* or *cwn-1; cwn-2* double mutants and completely lack the PLM polarity defects of *lin-44* mutant. Yet the *dpy-23* defects in HSN and QL migration are extremely severe. One explanation for these differences between *dpy-23* and *mig-14* mutants, as well as the differences between retromer and *mig-14* mutants, is that different Wnt-producing cells vary in their dependence on AP-2 or retromer to secrete Wnts. We speculate that endocytosis and retomer recycle MIG-14 for multiple rounds of Wnt secretion. If this hypothesis is correct, phenotypic differences could reflect the ability of some cells to synthesize sufficient MIG-14 resulting in less dependence on recycling. Alternatively, independent mechanisms for trafficking MIG-14 could operate in different Wnt-secreting cells.

EXPERIMENTAL PROCEDURES

Details on *C. elegans* genetics, molecular biology, β-galactosidase immunohistochemistry, and fluorescence confocal microscopy are available in the Supplemental Experimental Procedures.

Nomarski Microscopy for HSN Migration, Q Migration, and V5 Polarity

Positions of HSN and Q descendents were scored in newly hatched L1s and L1s 10–12 hr after hatching, respectively. Positions of HSNs were scored as previously described (Pan et al., 2006). QL migration was scored as defective when PVM and SDQL were positioned anterior to the V4.p cell, which indicates that the QL descendents migrated toward the anterior—the wrong direction. QR migration was scored as defective when AVM and SDQR were positioned posterior to V2.p, which indicates undermigration. The polarity of V cells were identified by Nomarski optics and confirmed with a GFP reporter the *jcIs1[ajm-1::gfp]* that labels adherens junctions (Koppen et al., 2001).

ALM and PLM Axon Scoring

Neuronal polarity of ALM and PLM was scored using the integrated array *zdIs5[Pmec-4::gfp]*, which is expressed in the six mechanosensory neurons ALMs, PLMs, AVM, and PVM. For ALM, the bipolar phenotype was defined as a normal anterior process and a posterior process that is longer than ten ALM cell diameters in length. For PLM, the symmetric phenotype was defined as a normal anterior process and a posterior process that extends to the tip of the tail. Reversed polarity was defined as an abnormally long posterior process that is longer than the anterior process, which is often truncated. In these cases, the posterior process reaches the tip of the tail, and then folds back to project anteriorly.

Supplemental Data

Supplemental Data include six figures and Supplemental Experimental Procedures and are available at http://www.developmentalcell.com/cgi/content/full/14/1/■■■/DC1/.

ACKNOWLEDGMENTS

We thank Andy Fire, Cynthia Kenyon, Hendrik Korswagen, and Lianna Wong for strains and reagents, and the *C. elegans* Genetics Center and the *C. elegans* Knockout Consortium for some of the strains used in this study. This work was supported by National Institutes of Health (NIH) grants NS32057 to G.G., NS034307 to E.M.J., and NS39397 to S.G.C. C.-L.P was supported by a Fellowship for Graduate Study from the Ministry of Education, Taiwan.

Received: October 5, 2007
Revised: November 9, 2007
Accepted: December 5, 2007
Published online: December 20, 2007

REFERENCES

Banziger, C., Soldini, D., Schutt, C., Zipperlen, P., Hausmann, G., and Basler, K. (2006). Wntless, a conserved membrane protein dedicated to the secretion of Wnt proteins from signaling cells. Cell *125*, 509–522.

Bartscherer, K., Pelte, N., Ingelfinger, D., and Boutros, M. (2006). Secretion of Wnt ligands requires Evi, a conserved transmembrane protein. Cell *125*, 523–533.

Bejsovec, A., and Wieschaus, E. (1995). Signaling activities of the *Drosophila* wingless gene are separately mutable and appear to be transduced at the cell surface. Genetics *139*, 309–320.

Coudreuse, D., and Korswagen, H.C. (2007). The making of Wnt: new insights into Wnt maturation, sorting and secretion. Development *134*, 3–12.

Coudreuse, D.Y., Roel, G., Betist, M.C., Destree, O., and Korswagen, H.C. (2006). Wnt gradient formation requires retromer function in Wnt-producing cells. Science *312*, 921–924.

Goldstein, B., Takeshita, H., Mizumoto, K., and Sawa, H. (2006). Wnt signals can function as positional cues in establishing cell polarity. Dev. Cell *10*, 391–396.

Goodman, R.M., Thombre, S., Firtina, Z., Gray, D., Betts, D., Roebuck, J., Spana, E.P., and Selva, E.M. (2006). Sprinter: a novel transmembrane protein required for Wg secretion and signaling. Development *133*, 4901–4911.

Harris, J., Honigberg, L., Robinson, N., and Kenyon, C. (1996). Neuronal cell migration in *C. elegans*: regulation of Hox gene expression and cell position. Development *122*, 3117–3131.

Hausmann, G., Banziger, C., and Basler, K. (2007). Helping Wingless take flight: how WNT proteins are secreted. Nat. Rev. Mol. Cell Biol. *8*, 331–336.

Herman, M. (2001). *C. elegans* POP-1/TCF functions in a canonical Wnt pathway that controls cell migration and in a noncanonical Wnt pathway that controls cell polarity. Development *128*, 581–590.

Hilliard, M.A., and Bargmann, C.I. (2006). Wnt signals and frizzled activity orient anterior-posterior axon outgrowth in *C. elegans*. Dev. Cell *10*, 379–390.

Koppen, M., Simske, J.S., Sims, P.A., Firestein, B.L., Hall, D.H., Radice, A.D., Rongo, C., and Hardin, J.D. (2001). Cooperative regulation of AJM-1 controls junctional integrity in *Caenorhabditis elegans* epithelia. Nat. Cell Biol. *3*, 983–991.

Liu, Y., Shi, J., Lu, C.C., Wang, Z.B., Lyuksyutova, A.I., Song, X.J., and Zou, Y. (2005). Ryk-mediated Wnt repulsion regulates posterior-directed growth of corticospinal tract. Nat. Neurosci. *8*, 1151–1159.

Lyuksyutova, A.I., Lu, C.C., Milanesio, N., King, L.A., Guo, N., Wang, Y., Nathans, J., Tessier-Lavigne, M., and Zou, Y. (2003). Anterior-posterior guidance of commissural axons by Wnt-frizzled signaling. Science *302*, 1984–1988.

Maloof, J.N., Whangbo, J., Harris, J.M., Jongeward, G.D., and Kenyon, C. (1999). A Wnt signaling pathway controls hox gene expression and neuroblast migration in *C. elegans*. Development *126*, 37–49.

Moline, M.M., Southern, C., and Bejsovec, A. (1999). Directionality of wingless protein transport influences epidermal patterning in the *Drosophila* embryo. Development *126*, 4375–4384.

Pan, C.L., Howell, J.E., Clark, S.G., Hilliard, M., Cordes, S., Bargmann, C.I., and Garriga, G. (2006). Multiple Wnts and frizzled receptors regulate anteriorly

directed cell and growth cone migrations in *Caenorhabditis elegans*. Dev. Cell *10*, 367–377.

Panakova, D., Sprong, H., Marois, E., Thiele, C., and Eaton, S. (2005). Lipoprotein particles are required for Hedgehog and Wingless signalling. Nature *435*, 58–65.

Prasad, B.C., and Clark, S.G. (2006). Wnt signaling establishes anteroposterior neuronal polarity and requires retromer in *C. elegans*. Development *133*, 1757–1766.

Seaman, M.N. (2005). Recycle your receptors with retromer. Trends Cell Biol. *15*, 68–75.

Seaman, M.N., McCaffery, J.M., and Emr, S.D. (1998). A membrane coat complex essential for endosome-to-Golgi retrograde transport in yeast. J. Cell Biol. *142*, 665–681.

Strigini, M., and Cohen, S.M. (2000). Wingless gradient formation in the *Drosophila* wing. Curr. Biol. *10*, 293–300.

Sulston, J.E., and Horvitz, H.R. (1977). Post-embryonic cell lineages of the nematode, *Caenorhabditis elegans*. Dev. Biol. *56*, 110–156.

Sulston, J.E., Schierenberg, E., White, J.G., and Thomson, J.N. (1983). The embryonic cell lineage of the nematode *Caenorhabditis elegans*. Dev. Biol. *100*, 64–119.

Tabata, T., and Takei, Y. (2004). Morphogens, their identification and regulation. Development *131*, 703–712.

Thorpe, C.J., Schlesinger, A., Carter, J.C., and Bowerman, B. (1997). Wnt signaling polarizes an early *C. elegans* blastomere to distinguish endoderm from mesoderm. Cell *90*, 695–705.

Walston, T., Guo, C., Proenca, R., Wu, M., Herman, M., Hardin, J., and Hedgecock, E. (2006). Mig-5/Dsh controls cell fate determination and cell migration in *C. elegans*. Dev. Biol. *298*, 485–497.

Whangbo, J., and Kenyon, C. (1999). A Wnt signaling system that specifies two patterns of cell migration in *C. elegans*. Mol. Cell *4*, 851–858.

Whangbo, J., Harris, J., and Kenyon, C. (2000). Multiple levels of regulation specify the polarity of an asymmetric cell division in *C. elegans*. Development *127*, 4587–4598.

White, J.G., Southgate, E., Thomson, J.N., and Brenner, S. (1986). The structure of the nervous system of the nematode *Caenorhabditis elegans*. Philos. Trans. R. Soc. Lond. B Biol. Sci. *314*, 1–340.

Yoo, A.S., and Greenwald, I. (2005). LIN-12/Notch activation leads to microRNA-mediated down-regulation of Vav in *C. elegans*. Science *310*, 1330–1333.

Yoshikawa, S., McKinnon, R.D., Kokel, M., and Thomas, J.B. (2003). Wnt-mediated axon guidance via the *Drosophila* Derailed receptor. Nature *422*, 583–588.

Zecca, M., Basler, K., and Struhl, G. (1996). Direct and long-range action of a wingless morphogen gradient. Cell *87*, 833–844.

Zou, Y., and Lyuksyutova, A.I. (2007). Morphogens as conserved axon guidance cues. Curr. Opin. Neurobiol. *17*, 22–28.

Developmental Cell *14*

Supplemental Data

C. elegans AP-2 and Retromer Control Wnt Signaling by Regulating MIG-14/Wntless

Chun-Liang Pan, Paul D. Baum, Mingyu Gu, Erik M. Jorgensen, Scott G. Clark, and Gian Garriga

Supplemental Experimental Procedures

Nematode Strains and Transgenic Animals

The following alleles or integrated arrays were used: *LGI*: *lin-44(n1792), lin-44(n2111), zdIs5[Pmec-4::gfp, lin-15(+)]*; *LGII*: *cwn-1(ok546), mig-14(ga62), mig-14(gm2)/mnC1, mig-14(mu71), mom-3(or78)/mnC1, vps-35(hu68), vps-35(zd163)*; *LGIII*: *mab-5(e1751*dm); *LGIV*: *egl-20(n585), jcIs1[ajm-1::gfp; rol-6(su1006)]*; *LGV*: *muIs3[Pmab-5::lacZ; rol-6(su1006)]*; *muIs49[Pegl-20::egl-20::gfp, unc-22 antisense]*; *LGX*: *dpy-23(e840), dpy-23(gm17)*. The following extrachromosomal arrays were used in this study: *gmEx450[Punc-86::dpy-23::gfp(1ng/μl), dpy-30::NLS::DsRed(50ng/μl)]*; *gmEx490[Pegl-20::dpy-23::gfp(50ng/μl), myo-2::gfp(50ng/μl)]*; *gmEx508[Pegl-20::mig-14::gfp, dpy-30::NLS::DsRed(25ng/μl)]*; *oxEx730[Pdpy-23::dpy-23::gfp, Punc-122::gfp]*; *oxEx753[Ppdi-2::dpy-23::gfp, Punc-122::gfp]*.

Molecular Biology and Germline Transformation

Standard molecular biology techniques were used to construct transgenes. To construct pCL5(*Punc-86::dpy-23::gfp*), a 5.1 kb fragment of the sequence upstream of the *unc-86* was isolated by PCR from genomic DNA and subcloned into pPD95.77 (obtained as a

gift from Andrew Fire). Transgenic animals injected with the resulting plasmid recapitulated the reported GFP expression pattern in HSN, Q neuroblast and other cells (data not shown). A *dpy-23* cDNA was obtained by RT-PCR and cloned between *Xma*I and *Kpn*I sites of the *Punc-86::gfp* plasmid. To construct pCL6 (*Pegl-20::dpy-23::gfp*), *dpy-23* cDNA was cloned between *Xma*I and *Kpn*I sites of pSK212, which contains a 1.9 kbp *egl-20* promoter sequence in pPD95.69 (Prasad and Clark, 2006). To construct *Pegl-20::mig-14::gfp*, a 8 kbp genomic *mig-14* fragment was amplified by PCR and cloned into *Kpn*I sites of pSK212. Germline transformation was performed by direct injection of various plasmid DNAs into the gonads of adult wild-type animals as described (Mello et al., 1991).

β-Galactosidase Immunohistochemistry

Animals containing the integrated array *muIs3[Pmab-5::lacZ]* were synchronized by hatching embryos in M9, feeding the larvae for 4 hours, and fixing them in cold acetone. β-galactosidase activity was assayed according to an established protocol (Maloof et al., 1999). Animals were countered stained with DAPI for better cell recognition. Worms were examined using a Zeiss Axioskop2 microscope. Images were acquired using a ORCA-ER CCD camera (Hammamatsu) and Openlab imaging software (Improvision). Images were prepared for using Adobe Photoshop (Adobe Systems).

Fluorescence Confocal Microscopy

Animals were immobilized with 1% sodium azide and observed with a Zeiss LSM510 confocal microscope. To determine the subcellular distribution patterns of MIG-14::GFP,

single confocal sections were taken through the center of the GFP-expressing cells. Four linear measurements of fluorescence intensity were taken from four axes (horizontal, vertical, two diagonal; see Figure S6) using LSM 5 Image Examiner (Zeiss). A peripheral distribution was defined as a fluorescence intensity on the cell membrane that was more than two fold the highest intracellular fluorescence intensity in three out of the four measurements (Figure S6A). An intracellular distribution was defined as the peak intracellular fluorescence intensity that was more than two fold the fluorescence intensity of the cell membrane in three out of the four measurements (Figure S6C). Conditions other than the two patterns described above were defined as an intermediate distribution (Figure S6B).

Supplemental References

Maloof, J.N., Whangbo, J., Harris, J.M., Jongeward, G.D., and Kenyon, C. (1999). A Wnt signaling pathway controls hox gene expression and neuroblast migration in C. elegans. Development *126*, 37-49.

Mello, C.C., Kramer, J.M., Stinchcomb, D., and Ambros, V. (1991). Efficient gene transfer in C.elegans: extrachromosomal maintenance and integration of transforming sequences. EMBO J *10*, 3959-3970.

Pan, C.L., Howell, J.E., Clark, S.G., Hilliard, M., Cordes, S., Bargmann, C.I., and Garriga, G. (2006). Multiple Wnts and frizzled receptors regulate anteriorly directed cell and growth cone migrations in Caenorhabditis elegans. Dev Cell *10*, 367-377.

Prasad, B.C., and Clark, S.G. (2006). Wnt signaling establishes anteroposterior neuronal polarity and requires retromer in C. elegans. Development *133*, 1757-1766.

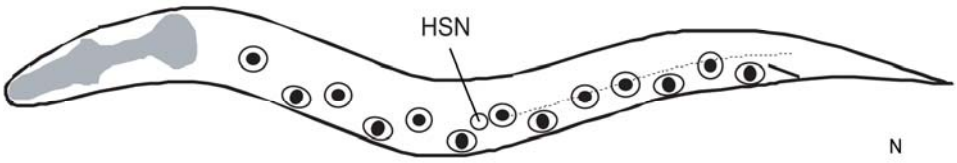

									N
wild type	100								50
egl-20	29	29	23	17		2			87
cwn-1; egl-20	2	5	27	36	10	12			59
lin-44; cwn-1;egl-20			13	18	16	20	12	20	60
dpy-23(e840)	2	5	6	13	11	29	9	25	55
dpy-23(gm17)			18	18	20	28	4	12	50
mig-14(mu71)		13	46	26	9	6			46
mig-14(ga62)		2	6	23	7	38	11	13	47
wild type	100								50
dpy-23(e840)	2	5	6	13	11	29	9	25	55
dpy-23; Pdpy-23::dpy-23	96	2	2						40
dpy-23; Ppdi-2::dpy-23	68	15	17						41
dpy-23; Punc-86::dpy-23		18	10	11	25	30	13	25	40
dpy-23; Pegl-20::dpy-23	29	42	23	6					31

Figure S1. Distribution of HSNs in Mutants and Transgenic Animals

The positions of HSN were scored as previously described (Pan et al., 2006). Numbers in boxes indicate the percentages of HSNs in defined positions, with gray scales corresponding to the percentages. N indicates the number of HSNs scored for each genotype. In wild-type animals, HSNs migrate to the interval between P5/6 and V4. In Wnt, *dpy-23* and *mig-14* mutants, the HSNs positions were shifted posteriorly. Mutations

in two Wnt genes, *lin-44* and *cwn-1*, significantly enhanced the HSN migration defects of *egl-20* mutants. The triple Wnt mutant of *lin-44; cwn-1; egl-20* had the most severe HSN migration defects. The severity of HSN defects in *e840* mutants, which lack *dpy-23*, is comparable to that of triple Wnt mutants, suggesting that *dpy-23* regulates multiple Wnt functions. Null mutations in *mig-14* are maternal-effect lethal. Mutants of *ga62* and *mu71*, two hypomorphic alleles of *mig-14*, are viable, but they have severe HSN migration defects, suggesting that zygotic MIG-14 function is required for proper HSN migration. Expression of DPY-23 from the *dpy-23*, *pdi-2* and *egl-20* promoters rescued the HSN defects of *dpy-23(e840)* mutants. The rescue from *egl-20* promoter is incomplete, reflecting the fact that HSN migration requires multiple Wnts.

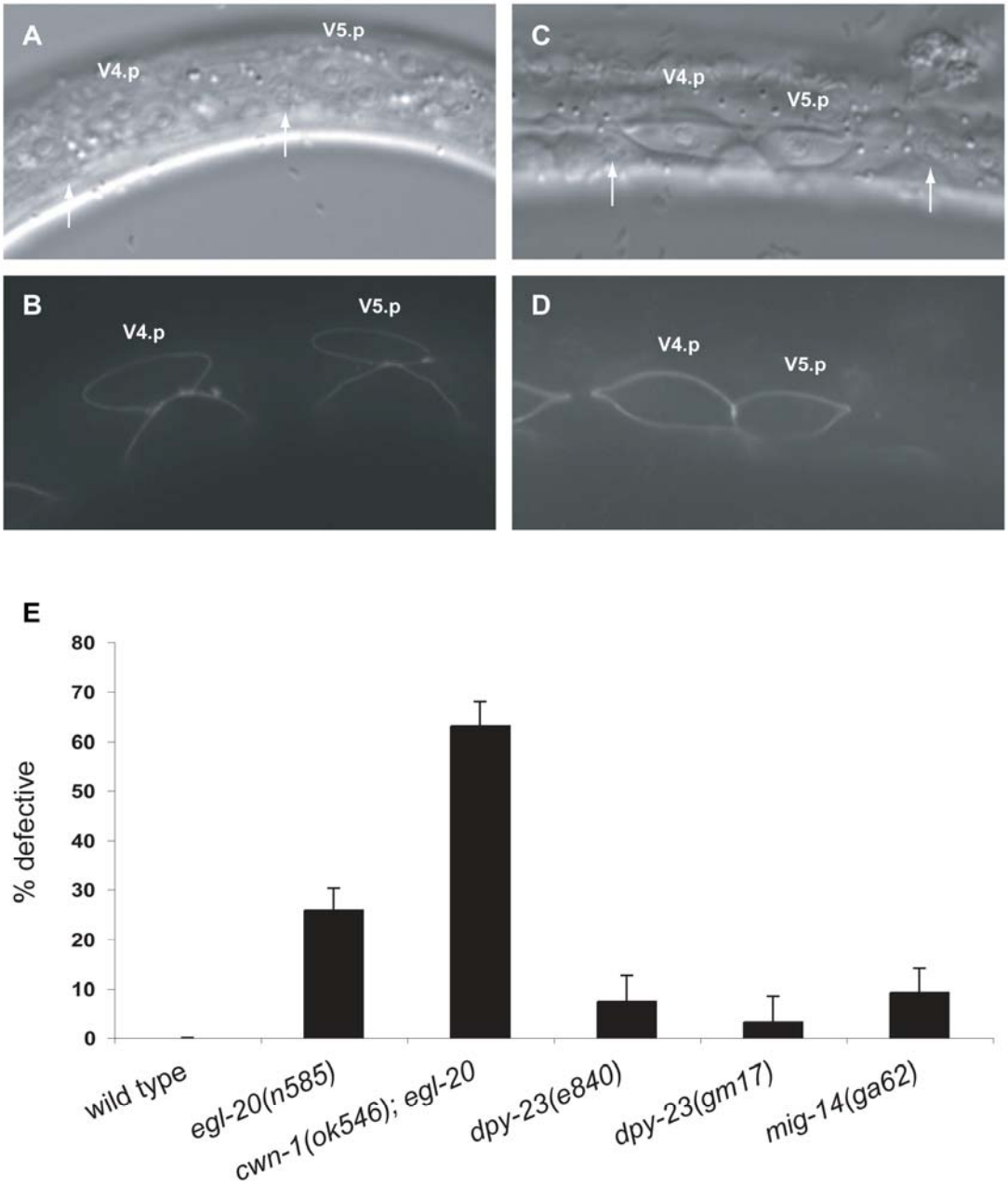

Figure S2. V5 Polarity Defects in Wnt, *dpy-23* and *mig-14* Mutants

(A-D) Photomicrographs of *jcIs1[ajm-1::gfp]* transgenic L1 larvae approximately four hours after hatching. V cells are visualized with Nomarski optics (A, C) and epifluorescence (B, D). *jcIs1* marks the adherens junction of epithelial cells. (A, B) Wild-

type L1. The anterior daughters of V cells become part of the hyp7 syncytium and only their nuclei could be seen (arrows) using Nomarski optics, whereas the posterior daughters become seam cells and retain their adherens junction, which is labeled by *ajm-1::gfp*. (C, D) *egl-20* L1. The division of V5 is reversed such that the anterior daughter becomes seam cell and retains the adherens junction, whereas the posterior daughter join the syncytium and loses its cellular boundary. Arrows mark the nuclei of V daughters that had fused with the hypodermal syncytium. (E) Quantification of V5 reversals in Wnt, *dpy-23* and *mig-14* mutants. The *cwn-1; egl-20* double Wnt mutants have much higher percentage of V5 reversals than the *egl-20* mutants. Both alleles of *dpy-23* and *mig-14(ga62)* show low percentages of V5 polarity defects. Numbers of animals scored for each genotype are: wild-type, 89; *egl-20*, 81; *cwn-1; egl-20*, 27; *dpy-23(e840)*, 68; *dpy-23(gm17)*, 62; *mig-14(ga62)*, 65.

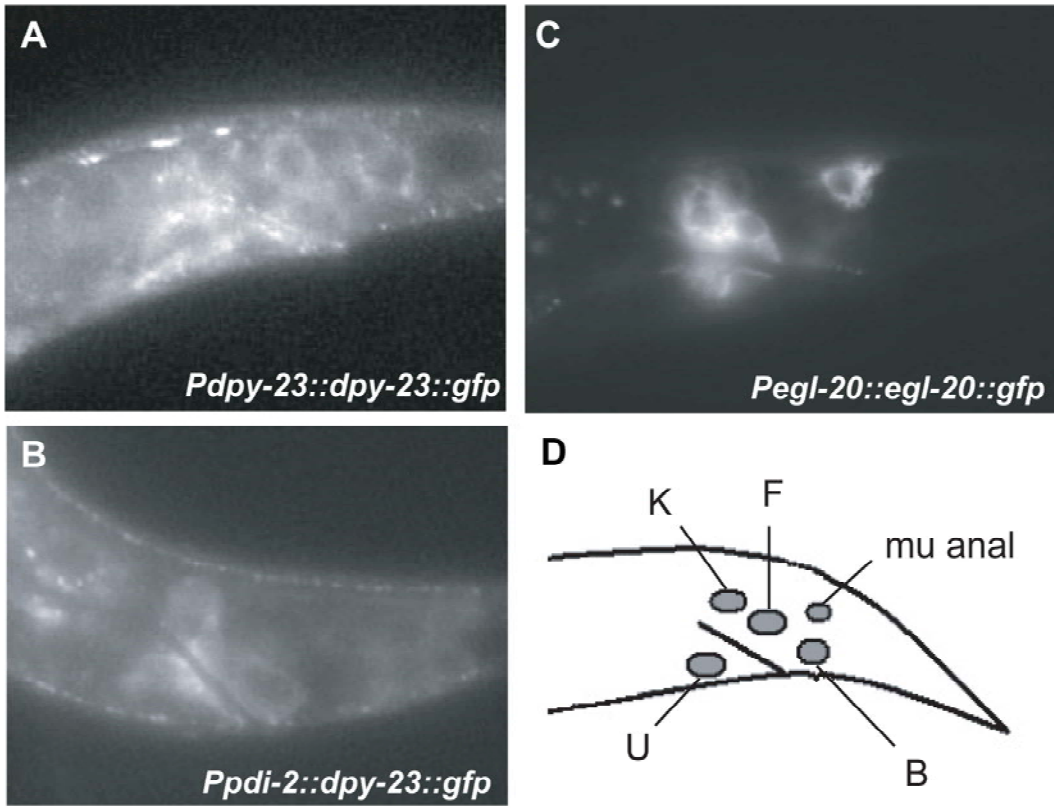

Figure S3. Expression Patterns of *dpy-23, pdi-2* and *egl-20* Promoters

The expression patterns of the *dpy-23* gene fused to GFP (A) and a *dpy-23::gfp* cDNA driven from the hypodermal cell promoter *pdi-2* (B) overlapped with that of the *egl-20::gfp* translational fusion (C) in a group of cells in the tail known to express *egl-20* (D).

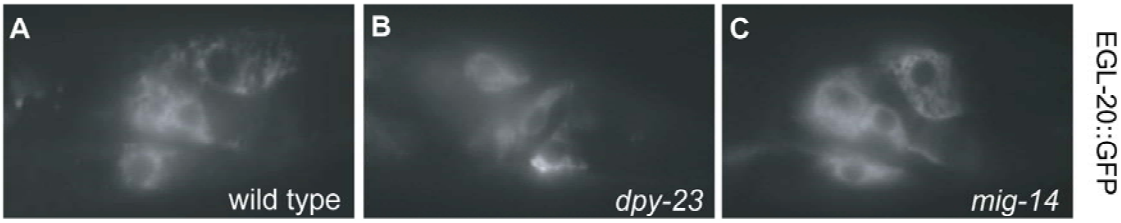

Figure S4. EGL-20/Wnt Expression in *dpy-23* and *mig-14* Mutants

Epifluorescence photomicrographs of EGL-20 expression in living animals, visualized with the integrated translational reporter *muIs49[egl-20::gfp]*. The EGL-20 expression level does not change in *dpy-23* and *mig-14* mutants compared to that of the wild type.

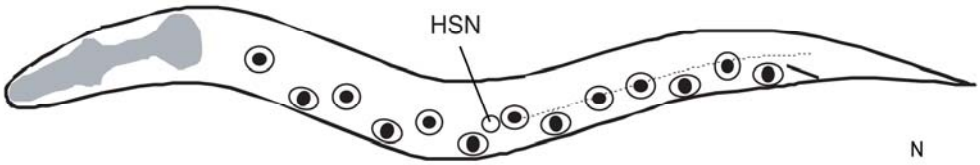

									N
wild type	100								50
mig-14(ga62)	2		9	20	20	35	6	13	54
mig-14(ga62); Pegl-20::mig-14	30	22	48						50
dpy-23(e840)			4	22	22	26	4	22	46
dpy-23(e840); Pegl-20::mig-14	7	7	45	17	10	10		3	29
dpy-23(gm17)			17	19	23	28	2	11	47
dpy-23(gm17); Pegl-20::mig-14	13	5	45	25	10	2			60
vps-35(hu68)	3		3	14	10	35	7	28	29
vps-35(hu68); Pegl-20::mig-14	23	12	29	18	12	6			17

Figure S5. Effects of Excess MIG-14 on HSN Migration in *dpy-23* and *vps-35* Mutants and in Neuronal Polarity in *mig-14* Mutants

HSN positions in *mig-14*, *dpy-23* and *vps-35* mutants with MIG-14 overexpression from the *egl-20* promoter. Numbers in boxes indicate the percentages of HSNs in defined positions, with gray scales corresponding to the percentages. N indicates the number of HSNs scored for each genotype.

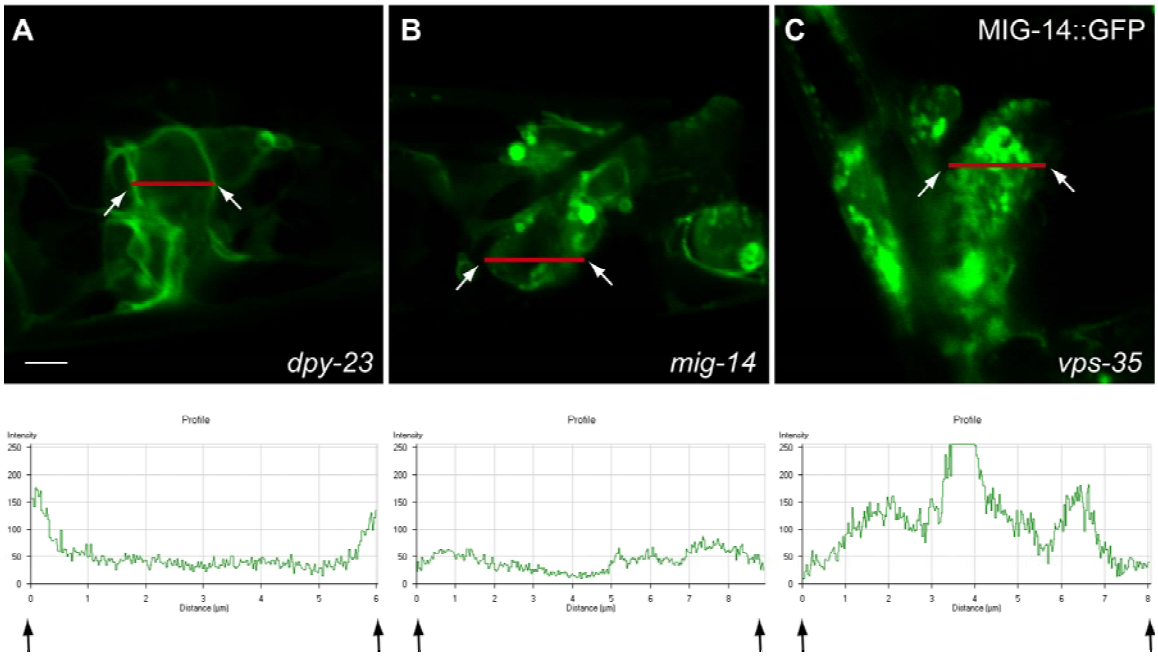

Figure S6. Measurement of MIG-14::GFP Fluorescence Intensities in EGL-20-Expressing Cells

Fluorescence confocal images of EGL-20-producing cells expressing MIG-14::GFP in *dpy-23 (A), mig*-14 (B), and *vps-35* (C) animals. Red lines indicate the measurement axes. White arrows indicate the positions of cell membranes, which serve as the starting and end points of the measurement. The lower panels showed the measurements of the fluorescence intensities. Black arrows correspond to positions of cell membranes in the upper panels. (A) Peripheral distribution: fluorescence intensities on the cell membrane were more than two fold of those inside the cell. (B) Intermediate distribution: fluorescence intensities on the cell membrane and inside the cells were variable. (C) Intracellular pattern: peak fluorescence intensities inside the cell were more than two fold of those on the cell membrane. Scale bar is 5 µm.